



Contents lists available at SciVerse ScienceDirect

## Brain Stimulation

journal homepage: [www.brainstimjrn.com](http://www.brainstimjrn.com)

## Original Research

Quantifying the effect of repetitive transcranial magnetic stimulation in the rat brain by  $\mu$ SPECT CBF scansTine Wyckhuys<sup>a,\*</sup>, Nele De Geeter<sup>b</sup>, Guillaume Crevecoeur<sup>b</sup>, Sigrid Stroobants<sup>a</sup>, Steven Staelens<sup>a,c</sup><sup>a</sup> Molecular Imaging Center Antwerp (MICA), Universiteitsplein 1, 2610 Wilrijk, University of Antwerp, Antwerp, Belgium<sup>b</sup> Department of Electrical Energy, Systems and Automation, Sint-Pietersnieuwstraat 41, 9000 Ghent, Ghent University, Ghent, Belgium<sup>c</sup> Medical Image and Signal Processing Group, De Pintelaan 185, 9000 Ghent, Ghent University-IBBT, Ghent, Belgium

## ARTICLE INFO

## Article history:

Received 23 May 2012

Received in revised form

19 September 2012

Accepted 11 October 2012

Available online xxx

## Keywords:

Repetitive transcranial magnetic stimulation

Regional cerebral blood flow

 $^{99m}\text{Tc}$ -HMPAO $\mu$ SPECT

Electric field distribution

## ABSTRACT

**Background:** Repetitive transcranial magnetic stimulation (rTMS) is used to treat neurological and psychiatric disorders such as depression and addiction amongst others. Neuro-imaging by means of SPECT is a non-invasive manner of evaluating regional cerebral blood flow (rCBF) changes, which are assumed to reflect changes in neural activity.

**Objective:** rCBF changes induced by rTMS are evaluated by comparing stimulation on/off in different stimulation paradigms using microSPECT of the rat brain.

**Methods:** Rats ( $n = 6$ ) were injected with 10 mCi of  $^{99m}\text{Tc}$ -HMPAO during application of two rTMS paradigms (1 Hz and 10 Hz, 1430 A at each wing of a 20 mm figure-of-eight coil) and sham. SPM- and VOI-based analysis was performed.

**Results:** rTMS caused widespread significant hypoperfusion throughout the entire rat brain. Differences in spatial extent and intensity of hypoperfusion were observed between both stimulation paradigms: 1 Hz caused significant hypoperfusion ( $P < 0.05$ ) in 11.9% of rat brain volume while 10 Hz caused this in 23.5%; the minimal  $t$ -value induced by 1 Hz was  $-24.77$  while this was  $-17.98$  due to 10 Hz. Maximal percentage of hypoperfused volume due to 1 Hz and 10 Hz was reached at tissue experiencing 0.03–0.15 V/m.

**Conclusion:** High-frequency (10 Hz) stimulation causes more widespread hypoperfusion, while 1 Hz induces more pronounced hypoperfusion. The effect of rTMS is highly dependent on the electric field strength in the brain tissue induced by the TMS coil. This innovative imaging approach can be used as a fast screening tool in quantifying and evaluating the effect of various stimulation paradigms and coil designs for TMS and offers a means for research and development.

© 2012 Elsevier Inc. All rights reserved.

## Introduction

Repetitive transcranial magnetic stimulation (rTMS) is an emerging method for the non-invasive stimulation of the human cortex through the intact skull. A rapidly changing perpendicular magnetic field is generated by the currents in a rTMS coil, but it is the induced electrical field in the conducting brain caused by this varying magnetic field (B-field) that triggers depolarization or hyperpolarization of neuronal ensembles, by forcing the shift of free charges in the intra- and extracellular space of neuronal tissue [1].

rTMS is a promising treatment for a variety of neurological and psychiatric disorders, such as depression, phantom pain and noise, ischemic stroke, neuropathic pain, migraine and Parkinson's disease [2–8]. Despite these promising results, the precise mechanism of action of rTMS and the pathways affected due to it are unknown. Furthermore, the optimal stimulation parameters and coil design are still undetermined, hampering its therapeutic potential. There is an innumerate number of degrees of freedom in terms of possible combinations of stimulation frequency, duration, intensity, coil design, stimulation pattern, brain target etc. emphasizing the need for a fast research, development and screening tool in the evaluation of rTMS' neurophysiological effect of each of these parameters. Human studies are restricted due to ethical considerations, the difficulty in gathering large and homogenous patient groups and the high costs. Therefore, to explore rTMS in a systematic, flexible and reliable manner, miniaturization of rTMS for rodent brain studies is

This study was financially supported by Ghent University, IBBT and the BOF-fund of the University of Antwerp.

**Conflict of interest:** The authors report no conflicts of interest.

\* Corresponding author. Tel.: +32 (0)3 265 28 19; fax: +32 (0)3 265 28 13.

E-mail address: [Tine.Wyckhuys@ua.ac.be](mailto:Tine.Wyckhuys@ua.ac.be) (T. Wyckhuys).

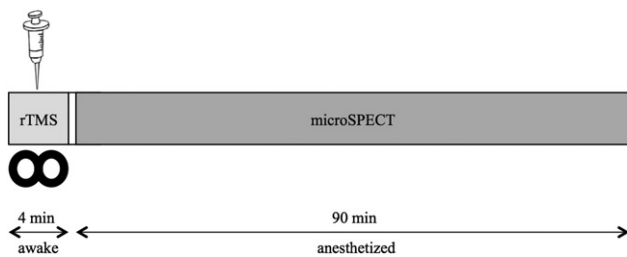


**Figure 1.** Protocol of one scan session. Before, during and after intravenous injection with 370 MBq  $^{99m}\text{Tc}$ -HMPAO, rats received continuous rTMS (1 Hz or 10 Hz) or sham, while awake. Then, rats were anesthetized following uptake of the tracer and  $\mu\text{SPECT}$  (1.5 h) was started.

an indispensable and complementary addition to the human studies.

Moreover, neuro-imaging by means of Single Photon Emission Computed Tomography (SPECT) is a non-invasive technique to evaluate regional cerebral blood flow (rCBF) changes, which are assumed to reflect changes in neural activity [9–11]. Intravenously injected  $^{99m}\text{Tc}$ -Hexamethylpropyleneamine oxime ( $^{99m}\text{Tc}$ -HMPAO) distributes rapidly (<2 min) within the brain, representing perfusion at the time of injection and is assumed to reflect neuronal and interneuronal activity downstream from cell bodies and in distant input pathways [9,12]. Consequently,  $\mu\text{SPECT}$  is a useful tool to indicate alterations in the local (inter)neuronal activity that is provoked by rTMS and can be used to evaluate changes induced by different rTMS-paradigms and coil designs. Recently, SPECT scanners have also been successfully miniaturized to enter the preclinical arena allowing for a high spatial resolution with an acceptable sensitivity in rats and mice ( $\mu\text{SPECT}$ ) [10,13,14].

In the current study, a voxel-of-interest (VOI)-based and statistical parametric mapping (SPM) analysis of stimulation-on versus stimulation-off (sham stimulation)  $\mu\text{SPECT}$  images was performed. Stimulation parameters were varied and effect on location, spatial extent and intensity of rCBF-changes were evaluated, in relation to the electrical field induced by the rTMS coil.

## Methods

### Animals

Male Wistar rats (250–300 g body weight; Harlan, the Netherlands) were treated according to guidelines approved by the

European Ethics Committee (decree 86/609/EEC). The study protocol was approved by the Animal Experimental Ethical Committee of Ghent University Hospital (ECP 04/08 complement). The animals were kept under environmentally controlled conditions (12 h normal light/dark cycles, 20–23 °C and 50% relative humidity) with food and water *ad libitum*.

### Experimental procedure

Before initiating the  $\mu\text{SPECT}$  scanning experiments, rats ( $n = 6$ ) were trained during one week to accustom to awake and comfortable positioning in a silicone rat head mold (cfr. Section 3.). After the behavioral training, all rats underwent three  $\mu\text{SPECT}$  scans. Each  $\mu\text{SPECT}$  scan was separated in time by at least 48 h for sufficient radioactive decay between scans. For each rat, the three stimulation paradigms (i.e. sham, 1 Hz and 10 Hz) were presented in a randomized order. For each of the  $\mu\text{SPECT}$  scans, rats were first shortly (max. 10 s) and lightly anesthetized with isoflurane (2% mixture with medical  $\text{O}_2$ ) to ensure accurate positioning of the head of the animal under the TMS coil in the silicone rat mold (cfr. Section 3.). Minimum 5 min was allowed between the arousal from anesthesia and the initiation of rTMS or sham. After 2 min of rTMS or sham stimulation, rats were, while awake and still under the silicone mold, intravenously injected with 370 MBq  $^{99m}\text{Tc}$ -HMPAO (Cereteq, GE Healthcare, UK). Stimulation was not interrupted during injection and was continued during the entire uptake of the  $^{99m}\text{Tc}$ -HMPAO tracer (for at least 2 min) following injection. After discontinuation of stimulation (or sham), rats were removed from the silicone mold and anesthetized with a mixture of isoflurane (2–5% isoflurane and  $\text{O}_2$ ) and placed onto the bed of the scanner. Body temperature was kept constant with a heating resistance mat and respiration frequency was measured throughout the duration of the  $\mu\text{SPECT}$  scan. The experimental protocol is illustrated in Fig. 1.

### Positioning of the TMS coil

Fixed position of the TMS coil in relation to the rat brain was ensured by using a custom-made silicone-mold (Belosil, Equator, Belgium), with an impression of the TMS coil at one side and an impression of the rat head at the other side (Fig. 2). The center of the TMS coil was positioned  $\pm 0.5$  cm to the left,  $\pm 0.5$  cm anterior to bregma and the distance between the coil and the rat's head was kept as small as possible without there being direct contact between skin and coil ( $\pm 0.5$  cm).

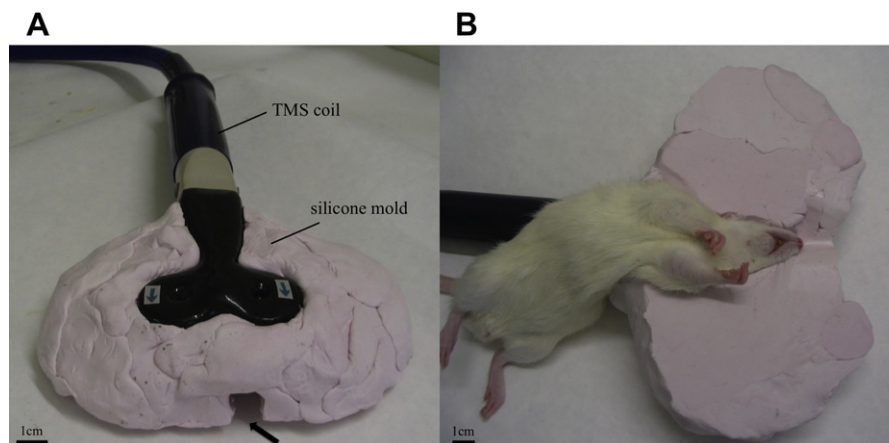


**Figure 2.** To ensure the exact position of the rTMS coil in relation to the rat brain, a silicone mold (pink) was used with an impression of the rTMS coil at one side (A) and an impression of the rat head at the other side (B). The animal was fully awake under the mold; therefore a breathing hole was foreseen (arrow). (For interpretation of the references to color in this figure legend, the reader is referred to the web version of this article.)

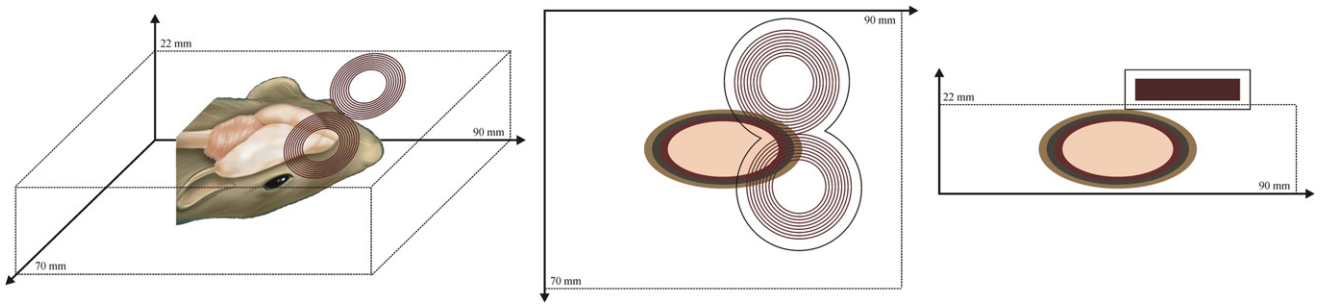


**Figure 3.** Position of the figure-of-eight coil and the rat in the field of interest. Axial and sagittal views of the modeled coil with coating and modeled rat head (ellipsoids).

The silicone mold tightly fits the rat's head: the animal is positioned in it while lightly anesthetized and is allowed to wake up while still being under the mold. Due to behavioral training, rats are minimally stressed while being under the mold and subsequently while receiving rTMS stimulation.

#### Transcranial magnetic stimulation

Transcranial magnetic stimulation was delivered with a Mag-Stim Rapid<sup>2</sup> stimulator (MagStim, UK). The smallest commercially available TMS coil, a figure-of-eight 20 mm coil (MagStim, UK), was used.

The parameters being delivered were i) trains of high-frequency 10 Hz, 50% of device power, 6 s duration and 54 s intervals and ii) continuous low-frequency 1 Hz, 50% of device power. The average number of pulses delivered was accordingly the same (60 pulses/min) in both stimulation paradigms. Sham stimulation was performed by positioning the rat in the silicone mold but with the coil positioned perpendicular and a few centimeters away from the skull and stimulating with a frequency of 1 Hz.

#### Imaging

##### $\mu$ SPECT

Dynamic multiframe scanning in 18 frames of 5 min was performed using the Milabs U-SPECT-II (MILabs, Utrecht, The Netherlands). This  $\mu$ SPECT scanner is equipped with collimators consisting of a tungsten cylinder with 5 rings of 15 pinhole apertures of 1.0 mm diameter. All pinholes focused on a single volume in the center of the tube. For imaging the rat's brain, the animal bed was translated in 3 dimensions using an XYZ stage into 8 different bed positions. A 20% main photopeak was centered at 140 keV to reconstruct the  $Tc^{99m}$  images. The data were reconstructed on 0.75 mm<sup>3</sup> voxels by 3 iterations of 16 Ordered-Subsets Expectation Maximization (OSEM) subsets [15].

##### MRI

In one rat (Sprague–Dawley, weighing 250 gr) MRI (3D T2-weighted) was performed on a 9.4 T MR system (Biospec 94/20 USR, Bruker Biospin, Germany). This image was used as a template for anatomical localization of perfusion maps.

##### CT

To enable the calculation of the position of the rTMS coil in relation to the rat brain, one microCT image was taken from the rat's head while in the silicone-mold. The detector has 3072 × 2048 pixels and may be configured for a FOV as large as 8.4 cm (transaxial) × 5.5 cm (axial). The X-ray source has a focal spot size of 50  $\mu$ m and measure in a voltage range of 35–80 kVp with a maximum anode current of 500  $\mu$ A. CT imaging was done using

a 220° rotation with 120 rotation steps. Voltage and amperage was set to 80 keV and 500  $\mu$ A, respectively. The rat head and silicone-mold was covered in 3 bed positions of 53.55 mm each with an overlap of 28.26% resulting in 130.4 mm axial FOV. Transaxial FOV is the same as the CCD readout in rat mode i.e. 82.12 mm. A good signal to noise ratio was obtained with pixel binning of 4 and an exposure time of 200 ms.

#### Induced electric field distributions under the TMS coil

The magnetic induction  $B(r, \omega)$  at location  $r$  produced by the current density  $J_{\text{coil}}(s, \omega)$ , with  $s$  being the location of the current in the coil with volume  $V$ , is calculated using Biot–Savart's law as in [16]:

$$B(r, \omega) = \frac{\mu_0}{4\pi} \iiint_V \frac{J_{\text{coil}}(s, \omega) \times (r - s)}{\|r - s\|^3} \cdot dv$$

with  $dv = dx_s dy_s dz_s$  an element of volume along the coil and  $\mu_0$  the permeability in vacuum.  $\omega = 2\pi f$  is the angular frequency in rad/s and  $f$  the frequency in Hz. The figure-of-eight coil (MagStim, UK) is modeled as two wings with 9 loops each and consists of rectangular copper wire (0.80 mm × 5.50 mm). The inner and outer radii of the loops are 4.35 mm and 13.15 mm respectively.

We measured the resulting voltage of this small coil at 50% output on the Rapid<sup>2</sup> stimulator (MagStim, UK). The voltage wave can be approximated by a sine with averaged peak amplitude of 28.6 V. Since the current transformer amounts 50 A/V, we can modulate the total excitation current as a sine with peak amplitude of  $I_a = 1430$  A in each wing, resulting in a current of 159 A and a current density of 36 A/mm<sup>2</sup> in each of the 9 wire loops.

The integration over the path along the coil of this current for the calculation of the corresponding magnetic induction is done using the Gauss–Legendre quadrature rule. The contribution of the second order magnetic induction originating from the eddy currents induced by the alternating first order magnetic field generated by the electrical coil current is neglected, since the order of magnitude of the induced currents is much smaller than  $J_{\text{coil}}$ , as previously published [16,17].

The rat head is modeled as four concentric ellipsoids representing the tissues scalp, bone, cerebrospinal fluid (CSF) and brain. The minor and major axes of the inner layer brain are 14 mm and 28 mm long and the other layers are 1 mm and 2 mm thick near the minor and major axes respectively, similar to the rat's real dimensions [18]. The exact positioning of the TMS coil was determined based on the microCT image containing the rat's head and the coil position relative to the head, with the figure-of-eight coil positioned in the axial plane, perpendicular to the skull, with its center 5 mm above the head model (Fig. 3). The head model and coil are surrounded by air. The isotropic material properties are obtained

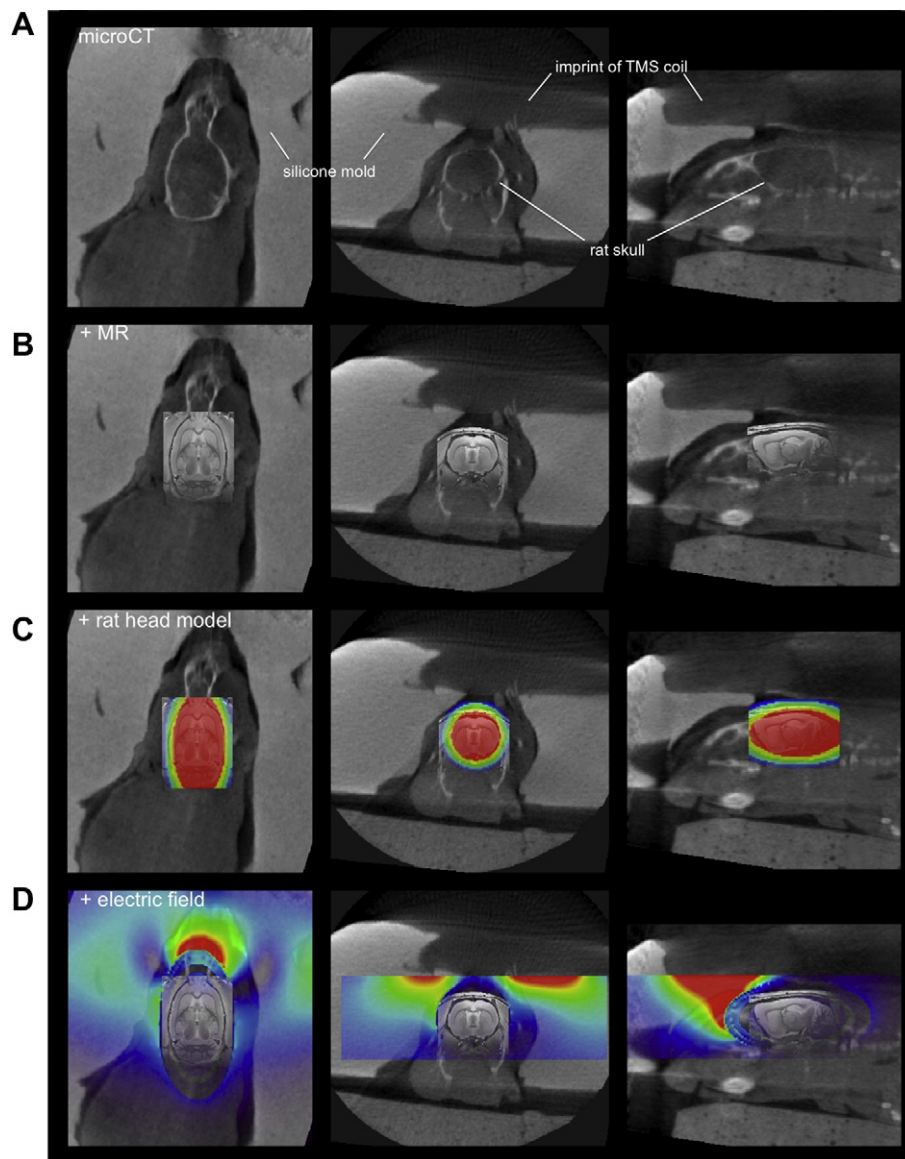


**Figure 4.** To exactly locate the rat brain areas with respect to the electric field induced by the TMS coil, a microCT image of the rat in the silicone mold was taken (A), revealing the rat skull in relation to the location of the TMS coil (by using the imprint of the coil in the silicone paste). Then, a 9.4 T MR image of the rat brain was overlaid onto the CT image using the rat skull delineation (B). The rat head model (ellipsoids) was positioned exactly on the microCT and MR images of the rat brain (C). Lastly, the electric field distributions were rotated under the TMS coil imprint and onto the rat head model (D).

from the 4-Cole–Cole model [19], whereby the brain is treated as grey matter.

The electric field, induced by the varying magnetic field generated by the coil current, is calculated using the recently developed independent impedance method [14]. Both the magnetic field and electric field distributions are calculated for a field of interest of  $30 \text{ mm} \times 50 \text{ mm} \times 22 \text{ mm}$  with a resolution of  $0.4 \text{ mm}$  as illustrated in Fig. 3.

#### *Coregistration of the induced electrical field distributions with the rat brain*

Firstly, the microCT image (Fig. 4A) of the rat in the silicone mold is used to manually coregister the 9.4 T MRI image of the rat brain using Amide (freeware; <http://amide.sourceforge.net>). This is straightforward and was performed by rotating the MRI image exactly within the boundaries of the skull, clearly visible at the microCT (Fig. 4B). The rat head model (four concentric ellipsoids)

was manually coregistered with the microCT image and MR of the rat in the silicone mold (Amide, Fig. 4C). The exact position of the TMS coil in relation to the rat head could be determined based on the imprint of the TMS coil in the silicone mold, visible on microCT. The distribution map of the modeled induced electric field was coregistered with the modeled rat head (Fig. 4D). As a result of previous coregistration steps, the rat brain areas (on MRI) were exactly located with respect to the induced electric field distribution map under the TMS coil as in Fig. 5 below.

#### *Data analysis*

To enable group comparisons between the stimulation paradigms, all data for all animals were spatially normalized into a common stereotactic atlas space – according to the Paxinos atlas for rat brain (PMOD v3.2, PMOD Technologies, Switzerland). First, the 9.4 T MRI rat brain image and the on/off  $\mu$ SPECT images were all transformed into the space of the ‘Rat (W. Schiffer)-T2’ and ‘Rat

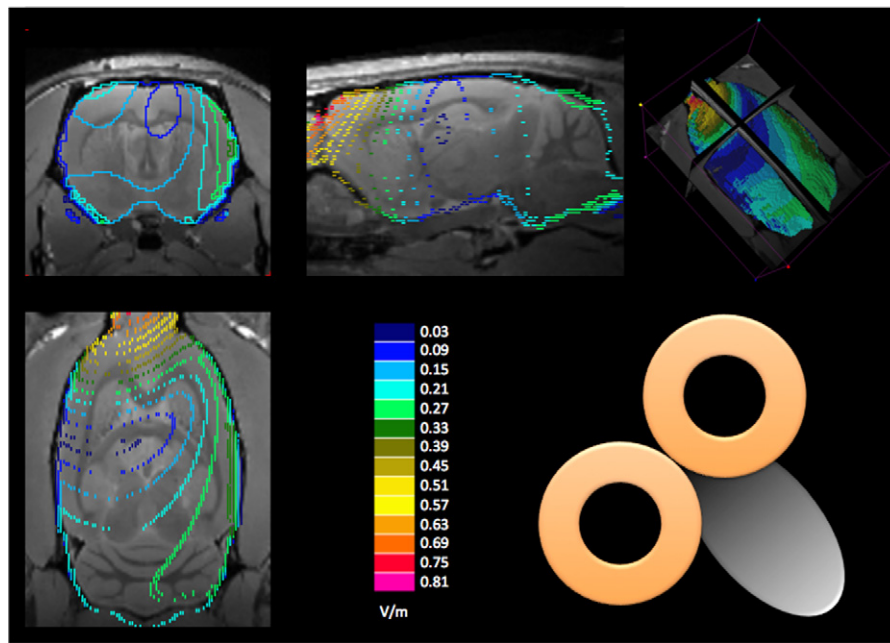


**Figure 5.** 9.4 T MR image of rat brain overlaid with VOI-map delineating the iso-values (here from 0.03 to 0.81 V/m) of the electric field strength generated by the rTMS coil and 3D rendering of VOI-map with schematic illustration of coil position in relation to the rat brain.

(W. Schiffer)-molecular imaging' template respectively, by brain normalization using the sum-of-squared-differences minimization algorithm and the 12-parameter affine transformation (PMOD v3.2, PMOD Technologies, Switzerland). Both existing templates are already into the same common space. We preferred a high-resolution 9.4 T MRI rat brain for anatomical reference in comparison to the lower-resolution 'Rat (W. Schiffer)-T2' atlas. Then, SPECT images were count normalized using a reference region. As large areas in the brain were assumed to be affected by TMS, we chose not to count normalize using whole brain uptake. The cerebellum is the brain structure most remote from the TMS coil and was presumed to experience the least influence from stimulation and was therefore chosen as reference structure: all voxel values of each  $\mu$ SPECT image were count normalized through dividing by the average activity concentration in the cerebellar structure. Spatially and count normalized images were masked to remove extracerebral activity.

To determine the overall degree of blood flow change, each individual SPECT image was overlaid on a predefined whole rat brain VOI template (PMOD v3.2). Values were averaged per condition (i.e. sham, 1 Hz and 10 Hz) and are indicated as percentage difference from baseline  $\pm$  SEM.

For SPM-analysis, images were smoothed (FWHM 3 times voxel size i.e.  $0.6 \times 0.6 \times 0.6$ ) and the hyper- and hypoperfusion T-map was achieved after paired analysis (stimulation vs sham) for both 1 Hz and 10 Hz (for each paradigm 6 pairs of data) using SPM8 (SPM8, Wellcome Department of Cognitive Neurology, London, UK). These T-maps were overlaid on the 9.4 T MR rat brain image (PMOD v3.2) and VOIs were calculated: i) a predefined VOI template, representing the major cortical and subcortical structures of the rat brain and ii) a VOI-map delineating by discretized iso-values of electric field strength, generated by the rTMS coil (Fig. 5). For each T-map, we determined the location, the maximal and minimal *T*-value, the total number of significant voxels (assuming  $P < 0.05$  to indicate significant differences; i.e. *T*-value  $> 2.015$  or *T*-value  $< -2.015$ ; degrees of freedom = 5) and correlated with the electric field strength using VOI-based analysis on the SPM parametric images. The percentage significant hypoperfused volume

per electric field-VOI was calculated as follows = volume of significant hypoperfusion per such VOI/total rat brain volume per such VOI.

## Results

No abnormal behavior was noticed during or following application of rTMS.

### General rCBF changes

Both 1 Hz and 10 Hz rTMS predominantly induce rCBF decreases (hypoperfusion). For the total rat brain, 1 Hz induced an overall decrease in blood flow of  $-5\% (\pm 3\%)$  while 10 Hz induced an overall decrease of  $-8\% (\pm 4\%)$  in comparison with sham stimulation. When SPM-images are analyzed, significant hypoperfusion was widespread throughout the entire rat brain (Figs. 6 and 7), both due to 1 Hz as 10 Hz. Overall, hypoperfusion due to 1 Hz stimulation was more restricted to cortical and dorsal subcortical areas, while 10 Hz stimulation also reached ventrally located subcortical structures. Significant bilateral hyperperfusion was only restricted to delineated structures involved in sensory information, mainly the auditory cortex, primary sensory cortex, the colliculus inferior, visual cortex and parietal cortex (Fig. 6). Also entorhinal cortex and retrosplenial cortex showed significant hyperperfusion.

### Intensity and spatial extent of rCBF changes

Low-frequency (1 Hz) stimulation induced an overall significant hypoperfusion of 11.9% (i.e.  $65 \text{ mm}^3$ ; total rat brain volume =  $600 \text{ mm}^3$ ) of the total rat brain, while high-frequency (10 Hz) stimulation induced an overall significant hypoperfusion of 23.5% (i.e.  $131 \text{ mm}^3$ ), which is 197% more than due to 1 Hz rTMS (Figs. 8 and 9).

For 1 Hz stimulation, the maximum percentage of significant hypoperfused electrical field VOI-volume (cfr. section 8) was reached where the electrical field strength was between 0.03 and 0.21 V/m, with its absolute maximum at 0.03–0.09 V/m (22.7% of

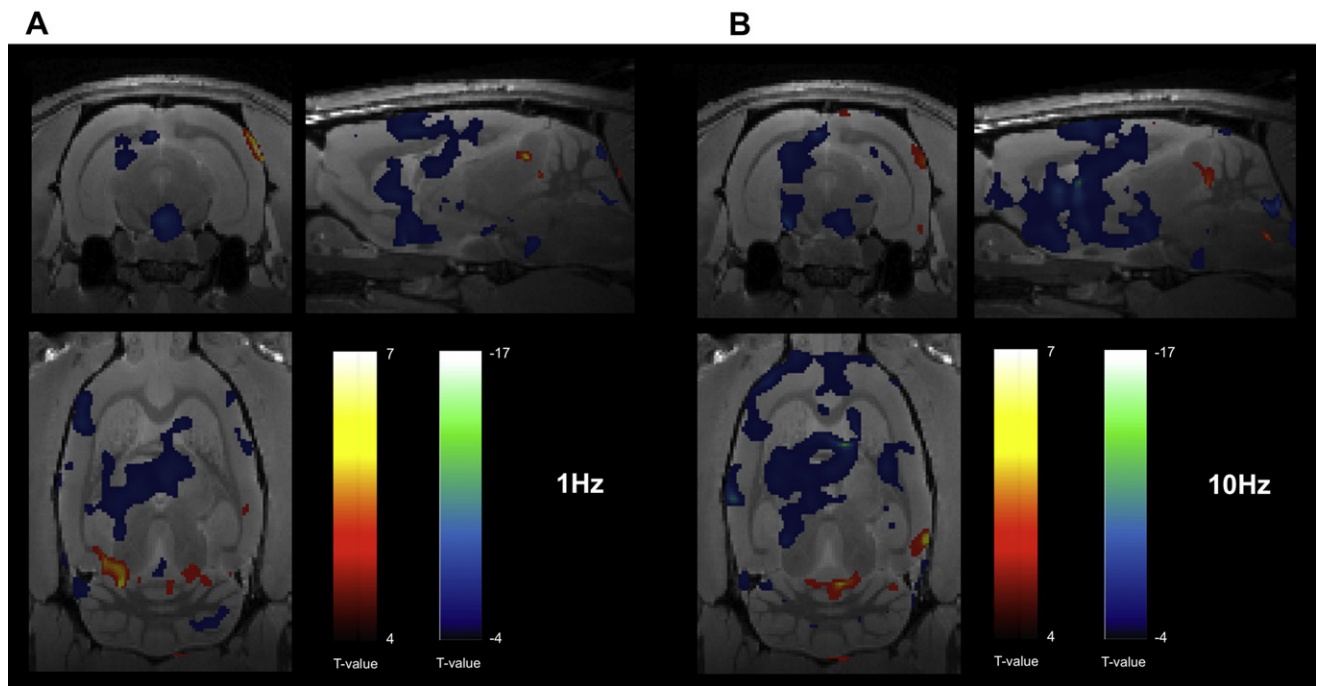


**Figure 6.** T-map with significant hyperperfusion (red) and hypoperfusion (blue) induced by 1 Hz (A) and 10 Hz (B) rTMS. Hyperperfusion is mainly restricted to areas involved in processing sensory information such as the auditory cortex, colliculus inferior, etc. Hypoperfusion is widespread throughout the entire rat brain, not restricted to delineated brain structures. (For interpretation of the references to color in this figure legend, the reader is referred to the web version of this article.)

that electrical isocontour VOI being significantly hypoperfused) (Fig. 9A). For 10 Hz stimulation, the maximum percentage was also reached where the field strength was between 0.03 and 0.09 V/m, with its absolute maximum at 0.09 V/m (36.8%) and a second maximum percentage was reached where electrical field strengths were between 0.33 and 0.57 V/m, with its absolute maximum at 0.33–0.39 V/m (34.7%) (Fig. 9A). This indicates that the lower the values of the induced electrical field, the more pronounced the maximal affected volume due to rTMS, for both 1 Hz and 10 Hz. A second maximum is reached for 10 Hz at higher induced electrical field values, while this is not the case for 1 Hz. Furthermore, these findings illustrate again the larger significantly hypoperfused volume induced by 10 Hz (36.8%) in comparison with 1 Hz (22.7%) in the peak region.

The minimal *T*-value for all significant hypoperfused voxels was  $-24.77$  for 1 Hz and  $-17.98$  for 10 Hz. The minimal *T*-value for 1 Hz was reached at 0.09–0.15 V/m (value  $-24.77$ ) (Fig. 9B). The minimal *T*-value for 10 Hz was also reached at tissue experiencing

0.09–0.15 V/m (value  $-17.98$ ) but also at tissue experiencing 0.27–0.33 V/m (minimal value  $-17.85$ ) (Fig. 9B).

## Discussion

In this study we demonstrated that repetitive TMS in rats, using the smallest commercially available human coil, caused a significant and widespread decrease in rCBF relative to sham stimulation. Two different stimulation paradigms i.e. low-frequency (1 Hz) and high-frequency (10 Hz) stimulation were evaluated and revealed a clear distinction in spatial extent and intensity of hypoperfusion between the stimulation paradigms. High-frequency stimulation induced a twice (197%) as widespread hypoperfusion in comparison with the low-frequency stimulation. Low-frequency stimulation induced however, more intense (with a minimal absolute *t*-value of  $-24.77$ ) hypoperfusion than 10 Hz stimulation (minimal absolute *t*-value  $-17.98$ ). Differences in location of induced hypoperfusion was observed for both paradigms: both 1 Hz and 10 Hz affected the

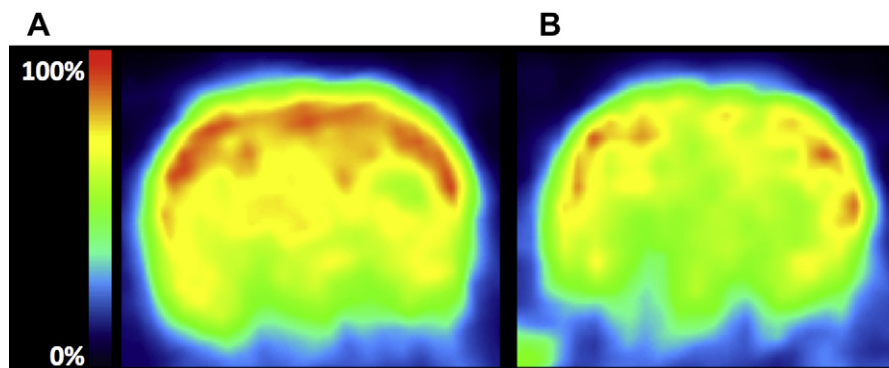


**Figure 7.** Coronal section of one representative rat during (A) sham stimulation and (B) 10 Hz TMS. Color bar represents relative intensity for  $^{99m}\text{Tc}$ -HMPAO. Note the lower uptake during 10 Hz stimulation in comparison with SPECT taken during sham stimulation.

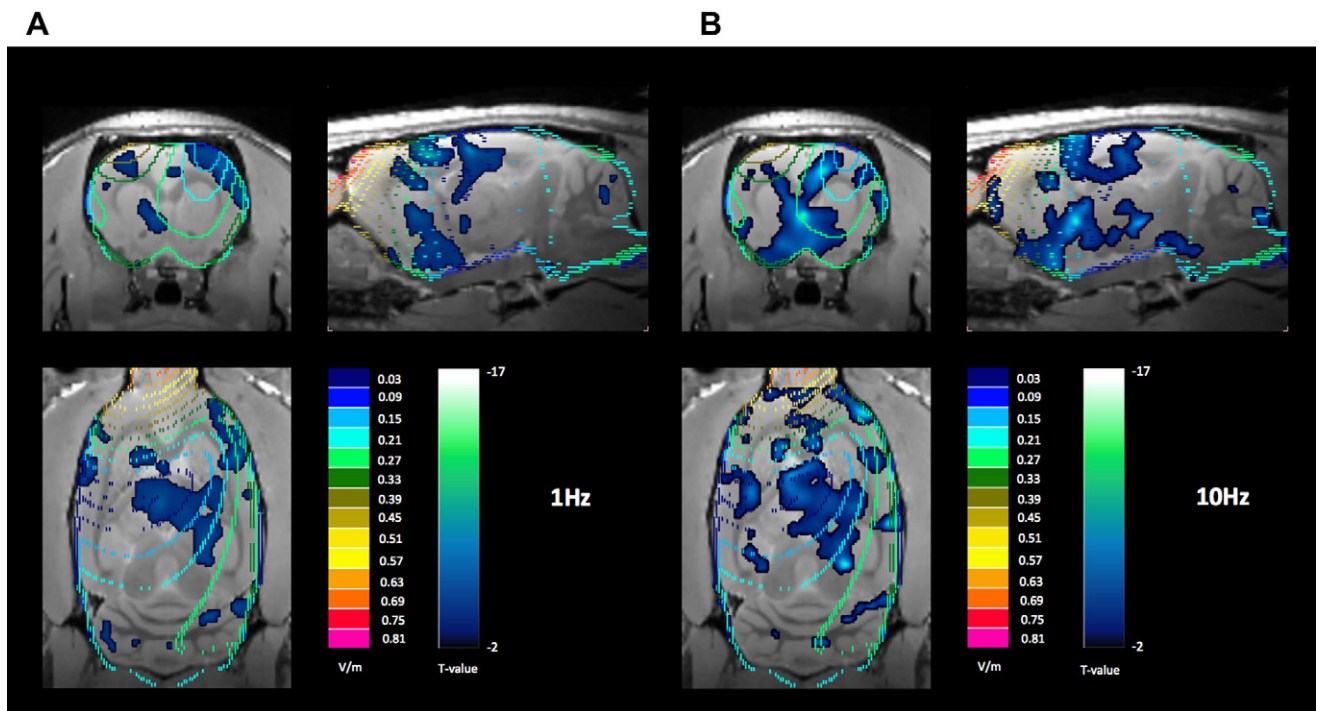


**Figure 8.** 9.4 T MR rat brain with overlay of hypoperfusion T-map (blue) and VOI-map of the electric field strengths (multi-colored) for 1 Hz (A) and 10 Hz (B) illustrating the difference in spatial extent of the effect induced by both stimulation paradigms of rTMS. (For interpretation of the references to color in this figure legend, the reader is referred to the web version of this article.)

most widespread and most intense brain tissue at low electric field strengths of 0.03–0.15 V/m, but 10 Hz induced a second maximum of hypoperfusion at tissue affected by electric field strengths of 0.27–0.39 V/m.

A small percentage of the tissue was consistently hyperperfused following both 1 Hz and 10 Hz stimulation. The areas showing hyperperfusion were mainly restricted to delineated brain structures involved in processing sensory information such as the auditory cortex, colliculus inferior, parietal cortex, primary sensory cortex, etc. Increased activity in the auditory cortex and colliculus inferior (which receives input for the auditory cortex) can be contributed to the experimental manipulations: rats are injected with the tracer while being awake, under a tight silicone mold during delivery of rTMS. The noise of the TMS coil's clicking sound was audible and causes activation in the auditory regions, as well as activation in regions involved in the integration of sensory information (sensory and parietal cortex). Rats were behaviorally trained during one week to accustom positioning in the silicone mold and the effective TMS procedure was then repeated three times (sham, 1 Hz and 10 Hz) for each rat, which might explain the hyperperfusion seen in retrosplenial and entorhinal cortex, which are involved in the recall of episodic information.

As aforementioned, the current study revealed predominantly decreases in rCBF in the rat brain due to application of both 1 Hz and 10 Hz rTMS, widespread throughout the entire rat brain and not restricted to delineated brain structures. This indicates that the currently used rTMS coil, which was the smallest commercially available coil (figure-of-eight, 20 mm), was not focal enough to pinpoint one specific brain area in the rat. This is consistent with the notion that rTMS in small animals, even with miniaturized coils, is restricted due to spatial selectivity of stimulation [20].

Intravenously injected  $^{99m}\text{Tc}$ -HMPAO distributes rapidly within the brain, representing perfusion at the time of injection. Whether the significant changes in rCBF observed in this study reflect alterations in local (inter)neuronal metabolism [21], changes in

activity of distant input pathways [22] and/or that rTMS is directly affecting the cerebrovascular system, remains to be elucidated.

Regarding the directionality of TMS' effect, the literature is inconclusive [23]. Although it was previously roughly stated that low-frequency rTMS (1–5 Hz) acts by functional inhibition of the targeted brain region and high-frequency stimulation (5–20 Hz) induced neuronal excitation [24], much controversy has risen recent years. Despite the extensive (mostly human) research however, no clear-cut consensus has been reached on the effects of various rTMS paradigms, due to a lack of systematic and well-controlled comparative, within-subject studies [23]. Even the slightest variation in experimental set-up (i.e. duration of stimulation, intensity of stimulation, stimulation pattern, type of coil, targeted brain area, different patient population, execution of a specific task etc.) can cause discrepancies between findings.

To our knowledge, the current animal study is the first to quantitate the neurophysiological response of different stimulation parameters within the same animal, in relation to the electric field induced by the rTMS coil. Our findings indicate that there is a relationship between the strength of the induced electric field and the spatial extent and intensity of the induced hypoperfusion following rTMS: for each of both stimulation paradigms, there is an electric field strength 'optimum', where the most widespread and most intense neurophysiological effect is pursued: for both 1 Hz and 10 Hz, this optimum field strength is between 0.03 and 0.15 V/m. For 10 Hz, there is a second optimum around 0.27–0.39 V/m. However, for human experiments, the intensity of the induced electric field under the coil is typically around 100 V/m [25] and has been described to be optimally around 150–180 V/m to trigger slow waves over the sensorimotor cortex [26]. Despite the relatively low induced electrical fields in our experiment, we nevertheless observe widespread significant changes in rCBF in the rat brain. Currently, no dedicated small animal TMS coils are commercially available. Up till now, researchers are restricted to use TMS coils used for human peripheral stimulation ([27] and our

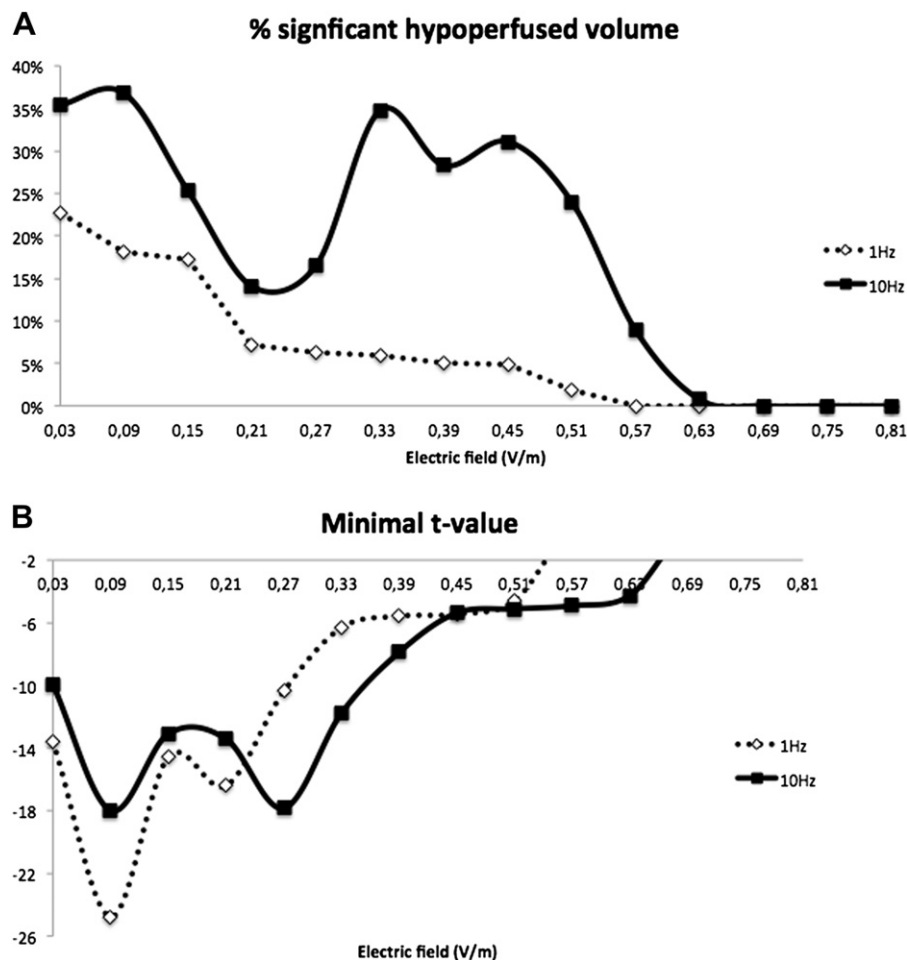


**Figure 9.** Graphs illustrating A) percentage tissue volume being significantly hypoperfused in relation to the electric field strength generated at the tissue due to 1 Hz (dotted line) or 10 Hz (full line); B) the minimal intensity of hypoperfusion induced by 1 Hz and 10 Hz, in relation to the electric field strength.

study) or large human brain TMS coils although dimensions of these coils and their respective magnetic and electric fields outreach the dimensions of the rodent's skull by far. Therefore, we developed an experimental small animal TMS coils and stimulators that might provide more flexibility for future animal research and that strives to deliver field strengths up to 120 V/m as in human applications although the current study indicates significant effects already at 0.03–0.09 V/m. Extensive numerical modeling studies however, are required to explore the optimal combination of coil geometry, size and orientation in relation to the animal's head to achieve focal stimulation in small animals especially due to the different ratio coil size/head size between animal and human [28]. Here again, molecular imaging can be of help in validating the numerical models and quantifying the focality of the induced electric fields.

Furthermore, our findings indicate that there is a substantial difference in neurophysiological effects between various stimulation parameters: 10 Hz causes more widespread hypoperfusion in comparison with 1 Hz, while 1 Hz induces more pronounced hypoperfusion. 10 Hz is also a more penetrant paradigm compared with 1 Hz as there is a second maximal effect in brain structures that are affected by higher electrical field strengths. This suggests that the intensity of the electric field at the tissue is crucial: the location of the maximal neurophysiological response following rTMS will be different depending on the choice of the stimulation paradigm and/or the choice of the stimulation intensity. To understand the resultant neural effects at each brain region

following rTMS, one also needs to keep in mind that i) the tissue under the TMS coil is not homogeneously distributed and inert, but involves white matter, grey matter, cerebrospinal fluid and various brain networks, each with its own characteristics such as preferred excitation threshold, difference in response time, inhibitory or excitatory connections with remote areas, ... leading to tissue-specific proneness to the electric field [29] and ii) the electric field itself can be deflected or attenuated when passing through each of these areas [30]. Electrophysiological measurements, such as multi-unit activity and local field potential recordings in the rodent brain as well as correlative physiological measurements such as motor evoked potentials during delivery of rTMS would be interesting in determining the exact underlying mechanisms behind the observed effects.

To our knowledge, this is the first report of an animal study using dedicated small animal *in vivo* molecular imaging as a fast screening tool in the visualization and quantification of rTMS paradigms. Previously, we already demonstrated that  $\mu$ SPECT was an innovative screening tool in the evaluation of experimental deep brain stimulation parameters [10]. Rodent rTMS studies so far, have only focused on indirect, invasive or terminal techniques such as motor-evoked potential (MEP) measurements [27,31], differences in cFOS mRNA or protein expression [32,33], manganese-enhanced MRI [34], microdialysis [35], behavioral changes [36,37], ... to study the effects of rTMS. Also, a numerical modeling study has investigated extensively the strength of the induced electric field in a modeled mouse brain caused by various commercially available

TMS coils [38], but no neurophysiological responses have been measured and correlated to the modeled electrical field strengths. More basic research is required through molecular imaging by systematically comparing the neural responses of different TMS parameter settings within the same subject, both for commonly used TMS protocols, as well as for experimental ones and to correlate it with the induced electrical field strengths. Furthermore, we are convinced that a great opportunity lays in the exploration of non-conventional stimulation parameters for rTMS. Commercially available stimulators are restricted in their choice of parameters but advances in TMS stimulator technology might make flexible choice in parameters for use in animal studies possible in the future.

## Conclusion

The current small animal study is the first to systematically quantitate the neurophysiological response of rTMS through molecular imaging and to relate it to the induced electric field strength induced by the TMS coil.

Ultimately, a better understanding of the neurophysiological effects of TMS and the screening of coils and stimulation paradigm parameters may lead to a better informed translation to clinical applications, resulting in more effective and well-controlled therapeutic interventions.

## Acknowledgments

Thanks to the Bio-Imaging Lab of the Antwerp University for the 9.4 T rat brain image.

## References

- [1] Barker AT, Jalinous R, Freeston IL. Non-invasive magnetic stimulation of human motor cortex. *Lancet* 1985;1(8437):1106–7.
- [2] Fitzgerald PB. The emerging use of brain stimulation treatments for psychiatric disorders. *Aust N Z J Psychiat* 2011 Nov;45(11):923–38.
- [3] Lipton RB, Dodick DW, Silberstein SD, Saper JR, Aurora SK, Pearlman SH, et al. Single-pulse transcranial magnetic stimulation for acute treatment of migraine with aura: a randomised, double-blind, parallel-group, sham-controlled trial. *Lancet Neurol* 2010;9(4):373–80.
- [4] Ridding MC, Rothwell JC. Is there a future for therapeutic use of transcranial magnetic stimulation? *Nat Rev Neurosci* 2007;8(7):559–67.
- [5] Topper R, Foltys H, Meister IG, Sparing R, Boroojerdi B. Repetitive transcranial magnetic stimulation of the parietal cortex transiently ameliorates phantom limb pain-like syndrome. *Clin Neurophysiol* 2003;114(8):1521–30.
- [6] Vanneste S, Plazier M, de Heyning PV, De Ridder D. Repetitive transcranial magnetic stimulation frequency dependent tinnitus improvement by double cone coil prefrontal stimulation. *J Neurol Neurosurg Ps* 2011;82(10):1160–4.
- [7] Khedr EM, Kotb H, Kamel NF, Ahmed MA, Sadek R, Rothwell JC. Longlasting antalgic effects of daily sessions of repetitive transcranial magnetic stimulation in central and peripheral neuropathic pain. *J Neurol Neurosurg Ps* 2005;76(6):833–8.
- [8] Khedr EM, Ahmed MA, Fathy N, Rothwell JC. Therapeutic trial of repetitive transcranial magnetic stimulation after acute ischemic stroke. *Neurology* 2005;65(3):466–8.
- [9] Shibasaki H. Human brain mapping: hemodynamic response and electrophysiology. *Clin Neurophysiol* 2008;119(4):731–43.
- [10] Wyckhuys T, Staelens S, Van Nieuwenhuyse B, Deleze S, Hallez H, Vonck K, et al. Hippocampal deep brain stimulation induces decreased rCBF in the hippocampal formation of the rat. *Neuroimage* 2010;52(1):55–61.
- [11] Matsuda H, Tsuji S, Shuke N, Sumiya H, Tonami N, Hisada K. Noninvasive measurements of regional cerebral blood-flow using Tc-99m hexamethylpropylene amine oxime. *Eur J Nucl Med* 1993;20(5):391–401.
- [12] Koyama M, Kawashima R, Ito H, Ono S, Sato K, Goto R, et al. SPECT imaging of normal subjects with technetium-99m-HMPAO and technetium-99m-ECD. *J Nucl Med* 1997;38(4):587–92.
- [13] Beekman FJ, van der Have F, Vastenhout B, Ramakers RM, Branderhorst W, Krah JO, et al. U-SPECT-II: an ultra-high-resolution device for molecular small-animal imaging. *J Nucl Med* 2009;50(4):599–605.
- [14] Cheng DF, Ruszkowski M, Pretorius PH, Chen L, Xiao N, Liu YX, et al. Improving the quantitation accuracy in noninvasive small animal single photon emission computed tomography imaging. *Nucl Med Biol* 2011;38(6):843–8.
- [15] Vastenhout B, Beekman F. Submillimeter total-body murine imaging with U-SPECT-I. *J Nucl Med* 2007;48(3):487–93.
- [16] De Geeter N, Crevecoeur G, Dupre L. An efficient 3-D eddy-current solver using an independent impedance method for transcranial magnetic stimulation. *IEEE T Bio-Med Eng* 2011;58(2):310–20.
- [17] Nadeem M, Thorlin T, Gandhi OP, Persson M. Computation of electric and magnetic stimulation in human head using the 3D impedance method. *IEEE T Bio-Med Eng* 2003;50(7):900–7.
- [18] Paxinos G, Watson C. The rat brain in stereotaxic coordinates. 6th ed. Academic Press; 2008.
- [19] Cole KS, Cole RH. Dispersion and absorption in dielectrics: alternating current characteristics. *J Chem Phys* 1941;9:341–51.
- [20] Funke K, Benali A. Modulation of cortical inhibition by rTMS – findings obtained from animal models. *J Physiol* 2011;589(18):4423–35.
- [21] Schwartz WJ, Smith CB, Davidsen L, Savaki H, Sokoloff L, Mata M, et al. Metabolic mapping of functional-activity in the hypothalamo-neurohypophyseal system of the rat. *Science* 1979;205(4407):723–5.
- [22] Ackermann RF, Finch DM, Babb TL, Engel J. Increased glucose-metabolism during long-duration recurrent inhibition of hippocampal pyramidal cells. *J Neurosci* 1984;4(1):251–64.
- [23] Reithler J, Peters JC, Sack AT. Multimodal transcranial magnetic stimulation: using concurrent neuroimaging to reveal the neural network dynamics of noninvasive brain stimulation. *Prog Neurobiol* 2011;94(2):149–65.
- [24] Post A, Muller MB, Engelmann M, Keck ME. Repetitive transcranial magnetic stimulation in rats: evidence for a neuroprotective effect in vitro and in vivo. *Eur J Neurosci* 1999;11(9):3247–54.
- [25] Roth BJ, Saypol JM, Hallett M, Cohen LG. A theoretical calculation of the electric-field induced in the cortex during magnetic stimulation. *Electroen Clin Neuro* 1991;81(1):47–56.
- [26] Massimini M, Ferrarelli F, Esser SK, Riedner BA, Huber R, Murphy M, et al. Triggering sleep slow waves by transcranial magnetic stimulation. *Proc Natl Acad Sci U S A* 2007;104(20):8496–501.
- [27] Rotenberg A, Muller PA, Vahabzadeh-Hagh AM, Navarro X, Lopez-Vales R, Pascual-Leone A, et al. Lateralization of forelimb motor evoked potentials by transcranial magnetic stimulation in rats. *Clin Neurophysiol* 2010;121(1):104–8.
- [28] Weissman JD, Epstein CM, Davey KR. Magnetic brain-stimulation and brain size – relevance to animal studies. *Electroen Clin Neuro* 1992;85(3):215–9.
- [29] Pell GS, Roth Y, Zangen A. Modulation of cortical excitability induced by repetitive transcranial magnetic stimulation: influence of timing and geometrical parameters and underlying mechanisms. *Prog Neurobiol* 2011;93(1):59–98.
- [30] Radman T, Ramos RL, Brumberg JC, Bikson M. Role of cortical cell type and morphology in subthreshold and suprathreshold uniform electric field stimulation in vitro. *Brain Stimul* 2009;2(4):215–28, 228 e1–3.
- [31] Luft AR, Kaelin-Lang A, Hauser TK, Cohen LG, Thakor NV, Hanley DF. Transcranial magnetic stimulation in the rat. *Exp Brain Res* 2001;140(1):112–21.
- [32] Mix A, Benali A, Eysel UT, Funke K. Continuous and intermittent transcranial magnetic theta burst stimulation modify tactile learning performance and cortical protein expression in the rat differently. *Eur J Neurosci* 2010;32(9):1575–86.
- [33] Ji RR, Schlaepfer TE, Aizenman CD, Epstein CM, Qiu D, Huang JC, et al. Repetitive transcranial magnetic stimulation activates specific regions in rat brain. *Proc Natl Acad Sci U S A* 1998;95(26):15635–40.
- [34] Jiang XD, Fa ZQ, Zhang P, Wu WW, Wang ZJ, Huang FH, et al. Functional mapping of rat brain activation following rTMS using activity-induced manganese-dependent contrast. *Neurol Res* 2011;33(6):563–71.
- [35] Kanno M, Matsumoto M, Togashi H, Yoshioka M, Mano Y. Effects of acute repetitive transcranial magnetic stimulation on dopamine release in the rat dorsolateral striatum. *J Neurol Sci* 2004;217(1):73–81.
- [36] Fleischmann A, Prolov K, Abarbanel J, Belmaker RH. The effect of transcranial magnetic stimulation of rat-brain on behavioral-models of depression. *Brain Res* 1995;699(1):130–2.
- [37] Akamatsu N, Fueti Y, Endo Y, Matsunaga K, Uozumi T, Tsuji S. Decreased susceptibility to pentylenetetrazol-induced seizures after low-frequency transcranial magnetic stimulation in rats. *Neurosci Lett* 2001;310(2–3):153–6.
- [38] Salvador R, Miranda PC. Transcranial magnetic stimulation of small animals: a modeling study of the influence of coil geometry, size and orientation. *Embc: 2009 annual international conference of the IEEE engineering in medicine and biology society*, vols. 1–20. 2009:674–677.